2021 43rd Annual International Conference of the
IEEE Engineering in Medicine & Biology Society (EMBC)
Oct 31 - Nov 4, 2021. Virtual Conference

Contactless Heart Rate Variability (HRV) Estimation Using a Smartphone During Respiratory Maneuvers and Body Movement

Monay Mokhtar Shoushan, Bersain Alexander Reyes, Aldo Mejia Rodriguez, and Jo Woon Chong, Member, IEEE

Abstract— **Heart rate variability (HRV) has been extensively investigated as a noninvasive marker to evaluate the functionality of the autonomic nervous system (ANS). Many studies have provided photoplethysmography (PPG) as a surrogate for electrocardiogram (ECG) signal HRV measurements. Remote PPG (rPPG) has been also investigated for pulse rate variability (PRV) estimation but in controlled conditions. We remotely extracted PRV using a smartphone camera for subjects in static and lateral motion while their respiratory rate was set to three breathing rates in an indoor illumination environment. PRV was compared with ECG-based HRV as a gold standard. We tested our algorithms on five healthy subjects. The results showed high correlation for rPPG-based HRV by presenting means of standard deviation of normal-to-normal intervals (SDNN) and root mean square of successive heartbeat interval differences (RMSSD) correlation coefficient greater than 0.95 in rest and greater than 0.87 in motion. The error of mean low frequency over high frequency (LF/HF) ratio estimated from PRV was 0.13 in rest and 0.25 in lateral motion. Moreover, a statistically significant correlation was obtained between HRV and PRV power spectra and temporal signals for all performed tasks. The obtained results contributed to confirm that remote imaging measurement of cardiac parameters is a promising, convenient, and low-cost alternative to specialized biomedical sensors in a diversity of relevant experimental maneuver.**

I. Introduction

Continuous monitoring of human physiological data is essential in the healthcare hospitalization field. Meanwhile, early detection of cardiac illness enhances the clinical therapy and patients' recovery rates. Heart rate variability (HRV) analysis was introduced as a measurement of the variation of beat to beat in a specific sinus rhythm. It measures the regularity in the heartbeat periods and heart rate subtlety deviation. Heart rate (HR) fluctuations is controlled by the autonomic nervous system (ANS) which maintains the body balance. ANS encompasses sympathetic and parasympathetic nerve system. The former steps up the HR while the later reduces it. Their final effect is concluded in the HRV. Consequently, HRV was regarded as a promising marker for the autonomic activity and a valuable model in clinical ambulatory interventions to predict heart failure and mortality. In addition, HRV could also report diabetic nerve damage, or diabetic neuropathy. Numerous studies investigated the compelling relationship between cardiovascular mortality and ANS, e.g., it was proven that HRV is a strong predictor for cardiac mortality. It can be evaluated using: a) time domain methods, as statistical or geometrical metrics, b) frequency domain evaluation, as spectral components analysis, and c) non-linear methods. HRV cardiac data were conventionally obtained using electrocardiogram (ECG). However, due to the nuisance of the ECG recording setting, photoplethysmography (PPG) was introduced as an alternative prospective non-invasive means for measuring the cardiac pulse from the fingertip using an oximeter US Food and Drug Administration (FDA) approved device or even a smartphone. Then, Remote PPG (rPPG), or imaging PPG (iPPG), recordings emerged to contribute to revolutionary healthcare monitoring systems applications. Several studies, as in [1, 2], found that pulse rate variability (PRV) measurements extracted from PPG signal were highly correlated with those obtained from ECG-based HRV. Another approach was introduced to derive PRV from iPPG in [3] through facial videos and compare it with HRV features obtained from a sensor reference system for sitting subjects who were allowed for natural movements. Extracted RGB color signals were converted to Lab color space, then by employing Fast Fourier Transform (FFT), Independent Component Analysis (ICA), Principal Component Analysis (PCA), heart rate and inter beat intervals were obtained. Average standard deviation of normal-to-normal intervals (SDNN) and low frequency over high frequency (LF/HF) were relatively close for HRV and PRV. In this paper, we propose a PRV features detection method for a smartphone-based iPPG in the presence of breathing activities with static or lateral motion. ECG-based HRV analysis was adopted as a gold standard. HRV from ECG and PRV from iPPG were derived from five subjects experiencing three respiratory rates: 6, 18, and 36 breath-per-minute (bpm), spontaneous breathing while in static position and the same three respiratory rates in lateral movement maneuvers. HRV and PRV parameters were compared for each task with same respiratory rate to investigate the monotonic agreement between them.

II. Materials and Methods

A. Data acquisition

iPPG signals were acquired from five healthy subjects' facial videos, 2 female and 3 males, their age range was from 21 to 25 years old. Videos were recorded for 120 seconds using a Samsung Galaxy S4 (Samsung, Seoul, South Korea) with 1920×1080-pixel image resolution and 30 frames per second (fps). They were either in static position or performing lateral movement, approximately 1 meter away from the smartphone camera under regular laboratory illumination. To induce the lateral movement, subjects were asked to move their body in a lateral direction, i.e., left to right, such that the

Monay Mokhtar Shoushan and Jo Woon Chong are with the Department of Electrical & Computer Engineering Texas Tech University, Lubbock, TX, 79409, USA (e-mail: monay.shoushan@ttu.edu; j.chong@ttu.edu). Bersain Alexander Reyes and Aldo Mejia Rodriguez are with the Faculty of Science, UASLP, San Luis Potosi, 78295, Mexico (e-mail bersain.reyes@uaslp.mx; aldo.mejia@uaslp.mx). *(Corresponding author: Jo Woon Chong.)*

978-1-7281-1178-0/21/$31.00 ©2021 IEEE

subject moves one step to the left and returns to the starting location in a repetitive fashion. The degree of movement varied for each subject. In the meantime, they were experiencing spontaneous breathing and 3 metronome breathing rates: M1=6, M3=18, and M6=36 bpm. Subjects were guided for respiratory maneuvers using a developed application which showed a bouncing ball at the required respiratory rate. Respiratory signals were synchronously acquired using Biopac piezoelectric sensor and were used to verify the subjects' actual breathing rate after the experiment procedure for each breathing metronome. Table I summarizes the performed tasks. The experimental procedures involving human subjects described in this paper were approved by the Institutional Review Board of Faculty of Science; Autonomous University of San Luis Potosi (UASLP) approved Institutional Review Board (IRB2018-197). ECG signals were measured using BIOPAC MP150 system (BIOPAC Systems Inc., Goleta, CA, USA) as a reference, simultaneously with iPPG signals acquisition. As a ground truth reference, ECG was used to evaluate the performance of our proposed iPPG-based PRV estimation by comparing its features with ECG-based HRV measures.

B. iPPG signal extraction

Raw color signals were extracted for each frame in a string of RGB video frames where the whole face was considered as a rectangular region of interest (ROI). Face was detected using Viola Jones and cascaded filters algorithm. This process will be followed by repetitive classification steps on the subsequent sub windows until the face image is detected. For filtering the non facial pixels, first, HSV masking was applied. HSV is a three dimensional color space that represents RGB color space in terms of:1) Hue (*H*): color type varying from 0-360 degrees, 2) Saturation (*S*): describes purity of color by the amount of mixed white color with the hue and represented as percentage from 0-100, 3) Value (*V*): defines the color brightness intensity and changes from 0-100.

The applied threshold ranges of upper and lower limits for *H,S, and V* were selected as in [4]: [0^o, 48°], [0.23, 0.62], and [0.44, 1], respectively.

Second, irrelevant pixels which did not satisfy the following equation were discarded:

$$|c^0(t) - c_{i,j}(t)| < \gamma\, \sigma_{ROI}(t), \qquad (1)$$

where $c^0(t)$ is the average raw color signal on a selected ROI, $c_{i,j}(t)$ represents the pixel with color value, γ is a multiplication factor that was set in our study to 1.5 and $\sigma_{\mathrm{ROI}}(t)$ is the standard deviation expressed as

$$\sigma_{\mathrm{ROI}} = \sqrt{\frac{1}{|\mathrm{ROI}(t)|}\sum_{(i,j)\epsilon \mathrm{ROI}(t)}(c_{i,j}(t) - c^0(t))^2}. \qquad (2)$$

For each ROI, we computed the average intensity of the red, green, and blue channels color signals. Each color signal was normalized across the signal interval by their mean to eliminate the light brightness effect [5]. A finite impulse response high-pass filter was applied for detrending the signals. To improve the signal smoothness, the signal was filtered using a moving average filter with M points which were selected to include the human pulse frequency range (0.65 and 4 Hz) [6].

POS model (plane-orthogonal-to-skin) was employed for $iPPG(t)$ signal extraction to account for the body motion ramification on the skin physiological reflections. Finally, re-applying MA filtration improved the final signal quality by eliminating the developed high frequency noise and artifacts from the nonlinear POS method. The processing tasks and data analysis were performed in MATLAB 2019a (MathWorks Inc., Natick, MA, USA).

B. iPPG signal Peak detection

PRV derivation is based on detecting iPPG signal peaks. We adopted our previous peak detection algorithm [4] to estimate HRV in this study. Peaks of the iPPG signal were defined as local maxima bounded by two successive minima, troughs. The peak amplitude is distinguished from a lower trough amplitude by a threshold value which is automatically calculated in the temporal domain. Fig. 1 represents a flow chart of the implemented methodology for iPPG signal extraction steps and reaching to PRV analysis.

C. ECG signal pre-processing and peak detection

For a noise free ECG signal, the baseline wander was suppressed using an infinite impulse response bandpass Elliptic filter. Then wave fiducial points (R) were detected via a MATLAB built-in function which locates the data local maxima.

D. HRV/ PRV analysis

Both signals time series, i.e., iPPG and ECG, were synchronized for HRV/PRV analysis. HRV was calculated from ECG successive R-wave peaks intervals or beat-to-beat intervals (RRI). For iPPG signal, with peaks counted as the maximum amplitude, the pulse to pulse signal interval (PPI) were used for the calculation of PRV measures. The recorded videos were considered as ultra-short-term since their epochs were less than 5 mins. In our study, to assess the agreement between PRV with HRV measurements we calculated the following standard parameters:

Time domain: estimated (SDNN) between detected beats interval, RRI or PPI, and root mean square of successive heartbeat interval differences (RMSSD).

Frequency domain: studies declared the reliability of the frequency domain features derived from ultra-short term HRV, however, there is still considerable uncertainty with regard to very low frequency (VLF) band features. Main spectral components were calculated for low frequency (LF=0.04 to 0.15 Hz), high frequency (HF=0.15 to 0.50 Hz), and (LF/HF). Cubic spline interpolation with 4 Hz resampled RRI and PPI series followed by the suppression of the DC component. Then, an autoregressive (AR) model of 12^{th} order was applied to estimate the power spectral density.

An additional feature, normalized root mean squared error (NRMSE), was calculated to evaluate the agreement between both power spectra and the time series signals and normalized it for each task as in the equation:

$$\mathrm{NRMSE}(\mathrm{x},\mathrm{y}) = RMSE/\bar{x}\,. \qquad (3)$$

TABLE I. TASKS DETAILS

Respiratory maneuver	*Movement condition*
M1 (6 bpm)	Rest / Lateral
M3 (18 bpm)	Rest / Lateral
M6 (36 bpm)	Rest / Lateral
Spontaneous	Rest

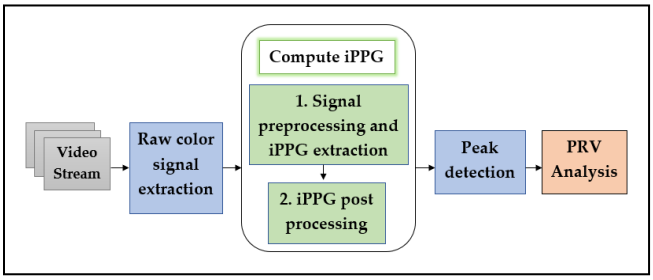

Figure 1. PRV processing flow chart.

The linear relationship was evaluated using Pearson's correlation coefficients (r) and the corresponding p-value for the autocorrelation signal matrix where (p-value < 0.05).

III. RESULTS AND DISCUSSION

HRV intervals were collected for a total of 70 minutes of recorded videos from 5 subjects performing 7 tasks. Each task represented a body position (rest or lateral motion) with a specific respiratory rate or a spontaneous breathing, as shown in Table I. Derived PRV indices for M1, M2, and M3 were compared to the ground truth, ECG-based HRV calculated indices. For all parametric measures, the outliers were identified by the 1.5xIQR rule and no outliers were identified. Pearson correlation were used to evaluate the metrics correspondence between HRV and PRV. Statistical correlation significance was also determined for all of the tasks regarding SDNN and RMSSD. After the correlation coefficients were calculated per task and per subject, the aggregated mean and standard deviation (SD) of the correlation coefficient were computed across all subjects for the same task, as shown in Table II. The SDNN minimum mean was 0.87 and maximum SD= 0.07. RMSSD significant correlation was reflected when aggregating their results. The minimum mean was 0.91 and maximum SD of 0.05.

Moreover, a significant correlation was found across temporal signals for most of the tasks when they were aggregated per task for all subjects. First, auto correlation was determined for each time series signal, all results were collected for HRV and PRV separately. Then, correlation was obtained between HRV and PRV autocorrelation results. Four of the tasks retuned correlation mean range of (0.93 – 1.0) and SD range of (0.0 – 0.07). However, two lateral motion tasks for M1 and M3 obtained lower mean of correlation coefficient and higher SD, as in Table II, (0.69±0.22) and (0.88±0.12) where subjects were breathing at 6 and 18 bpm, respectively. For M3 lateral correlation mean was considerably good (0.88) whereas M1 lateral associated correlation mean was low (0.69). One subject performing M1- lateral demonstrated high temporal correlation of (r = 0.99, p = 0.00). Correlation was low for the remaining four subjects performing the same task, correlation coefficient r range was (0.46 - 0.56) and significance p was lower than (0.03). This indicates that motion artifacts with low breathing rates affects the derived temporal signal correlation behavior. Also, the standard deviation of temporal correlation between PP and RR intervals for M1 were considerably high, denoting that the autocorrelation of temporal signals was not endorsing a linear relationship during lateral motion and breathing at 6 bpm. When applied the same previous correlation estimation method on the spectral power signals, the mean of correlation coefficients was significantly high for all tasks including the lateral motion tasks (range of 0.94- 0.99) with low SD range of (0.0-0.07), thus, a clear linear relationship was derived between PRV/HRV indices when analyzing the power spectrum signal. Fig. 2 shows boxplot of (NRMSE) calculated for the generated spectral power density from HRV and PRV signals for all subjects per task. No outliers were found, and the median varies in the range of 0.02 except for a task (M6 resting) where the difference increased to 0.06 between its median and the lowest median. Comparison of mean and SD of LF/HF were computed for all subjects per task, as in Table III. The error was evaluated for each subject per task then mean error was computed per task following the equation:

$$Mean\ error\ = Mean\left(\left|iPPG\frac{LF}{HF} - ECG\frac{LF}{HF}\right| / ECG\frac{LF}{HF}\right). \quad (4)$$

Lower error was identified in the comparison of mean LF/HF for static tasks than lateral tasks. This ratio represented the parasympathetic and sympathetic nerves balance. When the sympathetic function is dominant, the ratio is high, and the opposite when the parasympathetic is predominant [7]. The subjects in the experiment were standing and not resting whereas breathing metronomes were at specific set values, therefore, the resulted LF/HF were meaningful. For the spontaneous breathing task while standing, PRV and HRV metrics were analyzed and compared with M3-rest since in adults the normal respiration rate is 12–20 bpm [8] with average of 18 bpm, results are shown in Table IV. The following parameters were measured for both tasks : PRV/HRV SDNN correlation, PRV/HRV RMSSD correlation, LF/HF PRV, LF/HF HRV, Temporal HRV/ PRV correlation, Spectral HRV/ PRV correlation, NRMSE between PRV and HRV temporal signals, and NRMSE between PRV and HRV spectral signals. Then, mean and SD were calculated for all subjects of both tasks separately. Both tasks showed close mean values except for temporal correlation, was lower for the spontaneous breathing task (0.74). The rest of the correlation mean results were over (0.90).

Although low sampling rate could be a consideration for the smartphone HRV investigation, the pulse signals spectrum analysis demonstrated that the range of 0~10 Hz embraces the abundance of power [9].

IV. CONCLUSION

HRV is regarded for sustained physiological monitoring of cardiopulmonary diseases, sports training, and sleep studies. Conventionally, HRV observation requires physical contact.

TABLE II. FEATURES MEAN AND STANDARD DEVIATION ALL SUBJECTS PER TASK

Feature / Tasks	*SDNN Corr.*	*RMSSD Corr.*	*TIME Corr.*	*SPECT Corr.*
M1_Rest	0.98±0.03	0.99 ± 0.01	0.99 ± 0.0	0.98±0.03
M3_Rest	0.96±0.01	1.00 ± 0.00	0.93±0.05	0.99±0.01
M6_Rest	0.95±0.03	1.00 ± 0.00	0.95±0.07	0.99±0.00
M1_ Lateral	0.87±0.07	0.91 ± 0.05	0.69±0.22	0.96±0.05
M3_ Lateral	0.93±0.05	0.95 ± 0.04	0.88±0.12	0.94±0.07
M6_ Lateral	0.94±0.04	1.00 ± 0.00	1.00 ± 0.00	0.96±0.05
SPN_Rest	0.97± 0.03	1.00 ± 0.00	0.74±0.07	0.97±0.03

Many studies have proposed contactless HRV measurement, however, subjects were under controlled conditions. In this paper, we explore a potential feasible use for remote HRV monitoring during daily activities using a cost-effective and noninvasive available technology which can gauge the autonomic modulation.

We evaluated remote HRV, using a smartphone camera-based system, in different experiment modes. Subjects performed several tasks that were a combination of physical motion and breathing rate.

The experiment design presented many challenges as subjects' distance from smartphone, their body position, and body/motion artifacts, in the meantime, comparative results with employed reference were highly accurate. The spectral signals demonstrated more accuracy than the temporal ones.

A prime limitation to our study is the small number of subjects included. For future work, we plan to further assess the proposed approach on larger number of subjects with diverse data and in context of mixed motion conditions.

We consider that this and similar studies can facilitate incorporating remote HRV monitoring in sports monitoring protocols to evaluate players readiness and tolerance.

The proposed methodological approach is expected to embrace future development in the field of contactless HRV monitoring.

TABLE III. FEATURES MEAN AND STANDARD DEVIATION ALL SUBJECTS PER TASK

Feature / Tasks	*LF/HF iPPG*	*LF/HF ECG*	*Mean Error*
M1_Rest	1.62 ± 0.49	1.52 ± 0.12	0.15
M3_Rest	1.49 ± 0.11	1.27 ± 0.03	0.18
M6_Rest	1.48 ± 0.11	1.36 ± 0.06	0.08
M1_ Lateral	1.65 ± 0.42	1.38 ± 0.12	0.26
M3_ Lateral	1.53 ± 0.16	1.24 ± 0.07	0.23
M6_ Lateral	1.57 ± 0.32	1.26 ± 0.19	0.26

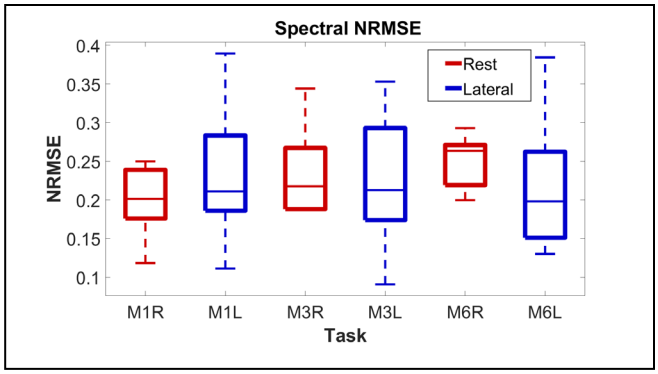

Figure 2. Boxplot of NRMSE measured for spectral signal difference between iPPG and ECG.

TABLE IV. RESTING (SPONTANEOUS / METRO_3) FEATURES COMPARISON ALL SUBJECTS

Feature	Mean ± STD	
	SPN_Rest	*M3_Rest*
SDNN Corr.	0.97±0.03	0.98±0.01
RMSSD Corr.	1.00±0.00	1.00±0.01
LF/HF PRV	1.62±0.21	1.49±0.11
LF/HF HRV	1.27±0.22	1.27±0.02
Temp. Corr.	0.74±0.07	0.93±0.05
Spec. Corr.	0.97±0.03	0.99±0.01
Temp. NRMSE	0.10±0.05	0.15±0.05
Spec. NRMSE	0.31±0.07	0.27±0.06

REFERENCES

[1] S. Lu *et al.*, "Can photoplethysmography variability serve as an alternative approach to obtain heart rate variability information?," *Journal of clinical monitoring and computing,* vol. 22, no. 1, pp. 23-29, 2008.

[2] M.-Z. Poh, D. J. McDuff, and R. W. Picard, "Advancements in noncontact, multiparameter physiological measurements using a webcam," *IEEE transactions on biomedical engineering,* vol. 58, no. 1, pp. 7-11, 2010.

[3] H. Rahman, M. U. Ahmed, and S. Begum, "Vision-based remote heart rate variability monitoring using camera," in *International Conference on IoT Technologies for HealthCare*, Springer, pp. 10-18, 2017.

[4] M. M. Shoushan, B. A. Reyes, A. M. Rodriguez and J. W. Chong, "Non-Contact HR Monitoring via Smartphone and Webcam during Different Respiratory Maneuvers and Body Movements," *IEEE Journal of Biomedical and Health Informatics,* vol. 25, no. 2, pp. 602-612, Feb. 2021.

[5] G. De Haan and V. Jeanne, "Robust pulse rate from chrominance-based rPPG," *IEEE Transactions on Biomedical Engineering,* vol. 60, no. 10, pp. 2878-2886, 2013.

[6] A. M. Unakafov, "Pulse rate estimation using imaging photoplethysmography: generic framework and comparison of methods on a publicly available dataset," *Biomedical Physics & Engineering Express,* vol. 4, no. 4, p. 045001, 2018.

[7] K. Takeshima *et al.*, "Central serous chorioretinopathy and heart rate variability analysis with a smartphone application," *Scientific Reports,* vol. 10, no. 1, pp. 1-8, 2020.

[8] T. Flenady, T. Dwyer, and J. Applegarth, "Accurate respiratory rates count: So should you!," *Australasian Emergency Nursing Journal,* vol. 20, no. 1, pp. 45-47, 2017.

[9] Lee, Chun T., and Ling Y. Wei. "Spectrum analysis of human pulse." *IEEE Transactions on Biomedical Engineering*, vol. 6, pp. 348-352, 1983.